Abluminal Stimulation of Sphingosine 1-Phosphate Receptors 1 and 3 Promotes and
Stabilizes Endothelial Sprout Formation

_____

A Thesis

Presented to

the faculty of the School of Engineering and Applied Science

University of Virginia

_____

in partial fulfillment

of the requirements for the degree

Master of Science

by

Steven Michael Lenz

December

2013

APPROVAL SHEET

The thesis

is submitted in partial fulfillment of the requirements

for the degree of

Master of Science

AUTHOR

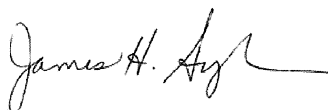The thesis has been read and approved by the examining committee:

Edward Botchwey

Advisor

Shayn Peirce-Cottler

Paul Yates

Accepted for the School of Engineering and Applied Science:

Dean, School of Engineering and Applied Science

December

2013

ABSTRACT

Local delivery of lipid mediators has become a promising new approach for therapeutic angiogenesis and regenerative medicine. In this study, we investigated how gradient stimulation (either abluminal/distal or luminal/proximal) of engineered microvessels with sphingosine 1-phosphate (S1P) receptor subtype-targeted molecules effects endothelial sprout growth using a microfluidic device. Our studies show distal stimulation of microvessels with FTY720, an S1P1/3 selective agonist, promotes both arterial and venular sprout growth, whereas proximal stimulation does not. Using pharmacological antagonists of S1P receptor subtypes, we further show that S1P3 functionality is necessary for VEGF-induced sprouting, and confirmed these findings *ex vivo* using a murine aortic ring assay in S1P3$^{-/-}$ deficient mice. S1P3 agonist stimulation enhanced vascular stability for both cell types via upregulation of the interendothelial junction protein VE-cadherin. Lastly, S1P3 activation under flow promoted arterial sprouting and branching while decreasing migratory cell fate in the microfluidic device. We used an *in vivo* murine dorsal skinfold window chamber model to confirm S1P3's role in neovascular branching. Together, these data suggest that a distal transendothelial gradient of S1P1/3-targeted drugs is an effective technique for both enhancing and stabilizing capillary morphogenesis in angiogenic applications.

KEY WORDS

Angiogenesis, sphingosine 1-phosphate, gradient directionality, S1P receptor subtype activation, endothelial barrier, microfluidic device

TABLE OF CONTENTS

CHAPTER 1: BACKGROUND

Angiogenesis, the biological formation of new blood vessels from existing ones, is central to many different diseases, disorders and pathologies including cancer,[1-5] peripheral artery disease[6-10] and ischemic stroke.[11-14] This process is influenced by a variety of soluble biomolecules, including growth factors (e.g. VEGF, PLGF, PDGF, TNFα, TGFβ, bFGF, and Ang 1),[15-18] matrix metalloproteinases,[19,20] chemokines (e.g. platelet factor-4),[21,22] and lipid mediators.[23-25] As small molecules, naturally occurring and synthetic lipid mediators such as sphingosine 1-phosphate (S1P) are receiving increasing interest in recent years as tools for developing pro-angiogenic and immunomodulatory regenerative medicine therapies, due to their relative stability and ease of use with regard to synthesis and delivery.[26-31] S1P signals through five G protein-coupled receptors designated S1P1-5, which vary in their downstream signaling effects including proliferation, migration and differentiation.[29,32] S1P1 and S1P3 are most heavily expressed on endothelial cells, while smooth muscle cells primarily express S1P3.[25] S1P is critical in the regulation of sprout formation, stabilization, and vessel permeability,[33-35] and numerous studies have shown that S1P works cooperatively with VEGF to regulate endothelial sprout formation and stabilization, via VE-cadherin.[34,36,37]

S1P is a blood-born lipid mediator that is responsible for a variety of physiological responses, most notably those in the immune and vasculature systems. Erythrocyte secretion maintains a high S1P concentration in the bloodstream (up to 1 µM), and thus there is a sharp concentration gradient between the blood and the surrounding tissue.[25,29,38] In both healthy physiology and disease states, S1P1 activation

induces immune cell migration of T and B lymphocytes, natural killer T cells, dendritic cells, macrophages, neutrophils, hematopoietic progenitors, mast cells and osteoclasts.[29] With regards to angiogenesis, S1P has been shown to either promote or inhibit vascular development depending on the receptor subtype stimulation.[25] Thus, the ability to activate specific S1P receptors is a promising strategy in developing novel angiogenic therapies.

Vascular endothelial growth factor (VEGF) is a homodimeric 34-42 kD glycoprotein that enhances vascular permeability as well as endothelial proliferation and differentiation.[39-42] VEGF-A is most heavily involved in angiogenesis and signals through the receptors Flt-1 (VEGFR-1) and Flk-1 (VEGFR-2), with approximately ten times the affinity for the former, although the latter has approximately ten times the tyrosine kinase activity.[39] In the wound healing cascade VEGF is secreted by activated platelets and induces a variety of cellular responses, including recruitment of circulating monocytes and bone marrow-derived endothelial progenitor cells to the injured site, endothelial invasion into the tissue, and pericyte stabilization of newly formed blood vessels.[39] In certain pathologies such as tumor growth beyond 2-3 mm^3, VEGF secretion not only sustains the supply of oxygen and nutrients to the tumor but also facilitates a means for malignant cells to enter the bloodstream and metastasize in distant tissues.[39] Thus, the balance between pro-angiogenic and anti-angiogenic factors is critical for maintaining healthy vascular development.

The interaction between S1P and known angiogenic growth factors has only recently become appreciated.[43-45] Together, S1P and VEGF have been shown to regulate transendothelial permeability, a critical component of endothelial sprout formation and

4

stabilization, via VE-cadherin.[25,46,47] VE-cadherin is a homophilic adherens junction protein expressed almost exclusively on the surface of endothelial cells.[36,37] When endothelial cells are stimulated with VEGF, VE-cadherin becomes phosphorylated and internalized via clatherin-coated pits, thereby increasing the permeability of the endothelial barrier.[36,48] In contrast, S1P stimulation inhibits the VEGF-induced signaling and stabilizes VE-cadherin localization at interendothelial junctions.[47] S1P1 and S1P3 stimulation independently promote VE-cadherin trafficking and adherens junction assembly via the non-Gi-dependent activation of the small GTPases Rac (through S1P1) and Rho (through S1P3).[47] While many have proposed a role for S1P in secondary or paracrine signaling between endothelial and stromal cells,[49,50] more recent studies suggest that its primary effects in the regulation of microvascular growth and remodeling are on endothelial cells themselves.[47,51]

In this work, we sought to study how gradient presentation of S1P receptor agonists effects endothelial cell morphogenesis. We chose FTY720 for its ability to specifically target S1P1 and S1P3. FTY720 is marketed as Fingolimod and has been approved by the Food and Drug Administration for treatment of multiple sclerosis. In addition, the S1P1 agonist/S1P3 antagonist VPC01091 was chosen to elucidate the relative importance of S1P3 in endothelial sprout formation. We have previously shown using a murine dorsal skinfold window chamber model that S1P3 activity is critical for increasing functional length density, vessel sprouting and recruitment of smooth muscle actin-positive cells to microvessels *in vivo*.[52] Ongoing studies in our lab are elucidating other effects of VPC01091 on the cellular content of peripheral blood.

A microfluidic device was determined to be an effective means of tightly controlling temporal, mechanical, and chemical cues within physiologically-relevant length scales. A 3-D microenvironment is preferred to a 2-D substrate because it allows for the formation of stable concentration gradients (unlike in well plates) as well as mechanical stimuli (such as fluid flow). Schaff et al. used a microfluidic device to study leukocyte rolling and adhesion to an endothelial monolayer under controlled flow and shear stresses.[53] van der Meer et al. co-cultured human endothelial cells and stem cell-derived pericytes within a microfluidic device to investigate the effects of TGF-β on vessel development, diameter and tortuosity.[54] Jeong et al. studied how VEGF gradients within a microfluidic device induced endothelial cell migration into an interpenetrating polymer semi-network HA-collagen hydrogel.[55] The particular microfluidic device used in this study consists of two parallel channels surrounding a central type-I collagen gel region, which is fixed by posts 100 µm apart. The spaces between these posts provide multiple sites where endothelial cells can attach and be easily imaged using confocal microscopy. The parallel channel system also allows for control over gradient directionality between the channels, as well as unidirectional fluid flow through the channels.[56,57]

Using this microfluidic device, we investigated how the directionality of S1PR agonist gradients and receptor subtype activation affect arterial and venular endothelial sprouting in a controlled microenvironment. We were able to show that S1P3 is required for VEGF-induced sprouting, which was confirmed *ex vivo* using an S1P3$^{-/-}$ aortic ring assay. Furthermore, distal S1P1/3 stimulation (and not proximal stimulation) promoted the greatest sprout growth, stabilization, and branching based on *in vitro* confocal

imaging and *in vivo* dorsal skinfold window chamber analysis. Together these results implicate that, independent of endothelial interaction with other blood or stromal cell types, the delivery method of S1P1/3 receptor-targeted drugs may be critical for improving angiogenesis both alone and in the presence of growth factors such as VEGF.

CHAPTER 2: METHODS

METHODS

Microfluidic Device

A two-channel microfluidic device (Fig. 1A) cast into PDMS (Dow Corning, Washington, D.C.) on silicon wafers was used for all experiments. Device fabrication, surface modification and measurements of gel regions are explained elsewhere.[56-59] The device used here has four ports for media (two for each channel) and two gel-filling ports. Briefly, the curing agent mixture was used in a 10:1 ratio, degassed in a vacuum chamber, then poured onto the master wafer and baked for 24 hr at 80 °C. After this the devices were punched to make media reservoirs and gel-filling ports and then wet/dry (20/10) autoclaved, followed by drying at 80 °C overnight. Devices were then plasma-bonded (Harrick Plasma, Ithaca, NY) to thin glass cover slides (Fisher Scientific). PDMS was used to block the port connecting the two media channels. This allowed cell seeding on only one side of the device, as well as ensured that diffusion of solutes from one channel to the other only occurred through the gel. After the devices were allowed to bake at 80 °C overnight, they were then filled with poly-D-lysine (Sigma-Aldrich, S. Louis, MO) and kept in the incubator at 5% CO_2 at 37 °C for 4 hr. Lastly, sterile molecular grade water was used to thoroughly wash each device twice before leaving them to dry in the oven at 80 °C overnight.

Gel Filling

2.5 mg/mL collagen (pH 7.4) was prepared by mixing 10 parts of 10x phosphate buffered saline (PBS), 17.2 parts of sterile water, 2.6 parts of 0.5 N NaOH and 70.2 parts

of 3.56 mg/mL collagen I (BD Biosciences, Bedford, MA) and titrated with minimal amount of 0.5 N NaOH. After being dried overnight, the devices were filled with 2.5 mg/mL collagen I and the gel was allowed to polymerize in a humidified incubator maintained at 37 °C under 5% CO_2 and 95% air for 1 hr. They were then filled with basal media (Angio-Proteomie, Boston, MA) and allowed to equilibrate overnight. Twenty-four hours after gel filling, green fluorescent protein (GFP)-expressing human umbilical vein or aortic artery endothelial cells (HUVECs or HAAECs) (Angio-Proteomie) were seeded as a monolayer on the collagen I gel.

Capillary Formation Assay

All cell cultures were maintained in a humidified incubator at 5% CO_2 and 37 °C. HUVECs or HAAECs were propagated in endothelial basal media (ENDO-Growth Kit, Angio-Proteomie) in 250 mL flasks coated with collagen I solution. Acetic acid solution (0.02 N) was prepared in water, filtered and sterilized, and collagen I solution (50 µg/mL) was prepared by adding 3.56 mg/mL collagen I (BD Biosciences) to the required volumes of the 0.02 N acetic acid solution. This was stored at 4 °C. Cell culture plates were coated with the collagen I solution and incubated at 37 °C for 3 hr.

Cells were seeded at a density of 2 x 10^6 per mL; 1 hr after seeding the cells in basal media (Angioproteomie), the media was replenished to ensure that all unattached cells were washed away. This was recorded as time point 0. At 24 h, the growth media was replaced by conditioned media (40 ng/mL VEGF [Life Technologies, Carlsbad, CA] or 250 nM S1PR agonist or the combination of VEGF and S1PR agonist). FTY720 was purchased from Cayman Chemical (Ann Arbor, MI). VPC01091 was generously

9

provided by Dr. Kevin Lynch in the Department of Pharmacology and Dr. Timothy Macdonald in the Department of Chemistry at the University of Virginia.

For static studies, conditioned media was changed every 12 hr. For flow studies, media solutions were loaded into syringes, and a syringe pump (World Precision Instruments, Sarasota, FL) was used to push the media at a constant flow rate of 1 µL/min through polyurethane tubing into the devices. For all such studies, flow in each channel had the same directionality.

Immunofluorescent Staining

After 6 days in vitro, cells were fixed using 4% PFA for 30 minutes and then stained for extracellular VE-cadherin expression. Devices were rinsed 3 times with wash buffer (5% bovine serum albumen [BSA] in 1X PBS) before incubating with block buffer (5% BSA + 10% goat serum in 1X PBS) for 2 hr at room temperature. Human VE-cadherin primary antibody (MAB9381, R&D Systems, Minneapolis, MN) was added at a concentration of 25 µg/mL in dilution buffer (1% BSA, 1% goat serum in 1X PBS) and devices were kept at 4 °C overnight. After washing 3 times (20 minutes each) with wash buffer, cells were incubated with the fluorescent-conjugated secondary antibody (NL008, R&D Systems) at a concentration of 1:100 in dilution buffer for 2 hr at room temperature. Devices were rinsed 3 times with 1X PBS and stored in the dark at 4 °C until imaged.

Imaging and Analysis

Cells were imaged 2, 4 and 6 days after seeding using confocal microscopy (Zeiss, Germany; Nikon EZ-C1 software, Melville, NY). Three devices were used for

each condition. Six gel regions (each defined as the region between two posts) from a device were randomly chosen for each of the conditions. Sprout density (i.e. number of sprouts per gel region) and number of individual cells migrating into the gel were calculated manually using ImageJ software package (National Institute of Health website, http://rsb.info.nih.gov/ij/). VE-cadherin expression was also quantified for cell monolayer and sprouts using ImageJ.

Mice

Animal experiments were performed using sterile techniques in accordance with an approved protocol from the University of Virginia Animal Care and Use Committee. All mice used were male and between 8-12 weeks and weighing between 18 and 25 grams. Wild type mice were C57BL/6 mice (Harlan, Indianapolis, IN), and S1P3$^{-/-}$ mice (a kind gift of Dr. Richard Proia [NIH]) were also on a C57BL/6 background.

Aortic Ring Assay

Male C57BL/6 mice (Harlan, Indianapolis, IN) or S1P$_3$$^{-/-}$ mice, age-matched and weighing between 18 and 25 grams were euthanized using IP injections of ketamine (80 mg/kg) and xylazine (8 mg/kg). In a supine position, the thoracic cavity was opened with scissors and the aorta was carefully lifted and excised from the mouse. The excised aorta was placed in cold sterile PBS. The periaortic fibroadipose tissue was carefully removed. With a sharp scalpel, the aorta was cut into rings (diameter ~ 1 mm) and rinsed extensively in consecutive cold sterile PBS washes. The rings were individually embedded in wells of a 24 well plate containing 300 µL synthetic basement membrane

(Matrigel; BD Biosciences). The rings were incubated for 30 minutes at 37 °C. 10 µM

VEGF was applied to the wells and the rings were incubated at 37 °C for 7 days. Images

of the rings were taken on a daily basis using a Zeiss inverted microscope to observe

growth. Quantification of the rings was done using ImageJ software.

Fabrication of PLAGA Thin Films

Poly-lactic-*co*-glycolic acid (PLAGA) thin films were fabricated using a solvent-

casting technique. 350 mg of PLAGA was combined with 2 mL of methylene chloride

(Fisher Scientific) in a borosilicate liquid scintillation vial (20 mL capacity, Fisher

Scientific) and vortexed until completely dissolved. The polymer solution was quickly

poured into a P35 petri dish (Nunc, area = 8.8 cm^2) lined with Bytac Teflon paper. Films

were allowed to dry at -20 ^{o}C for 7 days, and then stored at room temperature in a

desiccator until needed. All films were lyophilized (Labconco FreeZone 2.5, Labconco

Corp, Kansas City, MO) for 24 hours prior to being used for experiments in order to

remove any excess solvent. For implantation *in vivo*, films with a diameter of 1 mm were

extracted using a 1mm biopsy punch (Acuderm, Inc., Ft. Lauderdale, FL) and rinsed in

70% ethanol for ~30 seconds and then washed in sterile Ringer's solution for an

additional 30 seconds (137.9 mM NaCl, 4.7 mM KCl, 1.2 mM $MgSO_4$, 1.9 mM $CaCl_2$,

and 23 mM $NaHCO_3$). Films had an average thickness of 517±41 µm, as measured with

calipers (L.S. Starrett Co., Athol, MA).

Encapsulation of S1P Receptor-targeted Compounds in Polymeric Thin Films

FTY720 and VPC01091 were chosen as S1P receptor-targeted compounds. Films were loaded with a loading ratio of 1:200 (wt./wt., drug:PLAGA), 1.75 mg of drug was solubilized in 2 mL methylene chloride in a borosilicate scintillation vial using alternating cycles of heating (65 ^{o}C water bath) and vortexing until completely dissolved. 350 mg of 50:50 H-ME PLAGA was then added to the vial and the complete solution was vortexed until dissolved. The solution was slowly poured into a Teflon mold (area = 8.8 cm^2) and stored at -20 °C for a minimum of 7 days, or until needed for experiments. One day prior to experimentation, films with a diameter of 1 mm were extracted using a 1 mm biopsy punch (Acuderm, Inc.) and lyophilized for 24 hours to extract any remaining solvent (Labconco Corp., Kansas City, MO).

Dorsal Skinfold Window Chamber Surgical Procedure.

Mice were implanted with dorsal skinfold window chambers (APJ Trading Company, Inc., Ventura, CA). Mice were treated with a pre-anesthetic of atropine (0.08 mg/kg IP) and further anesthetized using intraperitoneal (IP) injections of ketamine (80 mg/kg) and xylazine (8 mg/kg). Dorsal skin was shaved, depilated, and sterilized using triplet washes of 70% ethanol and iodide. A double-layered skinfold was elevated off the back of the mouse and pinned down for surgical removal. The titanium frame of the window chamber was surgically fixed to the underside of the skinfold. The epidermis and dermis were removed from the top side of the skinfold in a circular area (diameter ~ 12 mm) to reveal the underlying vasculature. Exposed tissue was kept hydrated with sterile Ringer's solution (137.9 mM NaCl, 4.7 mM KCl, 1.2 mM MgSO$_4$, 1.9 mM CaCl$_2$, and 23 mM NaHCO$_3$). The titanium frame was then mounted on the topside of the tissue

and attached to its underlying counterpart. The dorsal skin was sutured to the two titanium frames and the exposed tissue was sealed with a protective glass window. Mice were allowed to recover in heated cages and subsequently administered buprenorphine via subcutaneous injection (0.1-0.2 mg/kg) as a post-operative analgesic. All mice received a laboratory diet and water *ad libitum* throughout the time-course of the experiment.

Implantation of Thin Films and Intravital Image Acquisition

PLAGA thin films were implanted into the window chamber 7 days post-surgical implantation, hereafter referred to as Day 0. Mice were anesthetized via 2% isoflurane mixed with 1 mL/min O_2. Subsequently, the glass window was removed to expose the thin layer of vessel networks. The window chamber was flooded with 1 mM adenosine in Ringer's solution (3 x 5 minutes) to maximally dilate all vessels and maintain tissue hydration. Following the last administration of adenosine, the solution was aspirated and two films (either both loaded or both unloaded) were placed equidistant from one another and from each edge of the window. The mouse was then mounted to a microscope stage and imaged non-invasively using a 4x objective on an Axioskop 40 microscope (Zeiss). Images were captured using an Olympus MicroFire color digital camera and PictureFrame image acquisition software (Optronics, Goleta, CA). Individual images were later photomerged into a single image of the entire microvascular network using Adobe Photoshop CS. Mice were initially imaged on Day 0 following film implantation and again on Day 3.

Quantitative Microvascular Metrics

Intravital microscopy montages of entire vascular windows at Day 0 and Day 3 were analyzed using a combination of Adobe Photoshop CS and ImageJ software packages for different treatment conditions. Circles with a diameter of 5 mm (or 2 mm concentric radius from outer edge of one film) were cropped around each film, with no overlap of the two circles. The number of venular branch points was quantified by marking a point of bifurcation on a blood vessel at days 0 and 3. This vessel branch was then followed and bifurcations were marked. These new branches were also tracked and marked at points of bifurcations; thus, branch points three degrees of freedom away from the parent vessel were quantified. The number of branch points at day 3 was normalized to the number present at day 0.

Statistical Analysis

Where appropriate, Student's t-test or Tukey's range test with a family confidence of 95% were used to calculate the statistical significance of different conditions on sprout metrics.

CHAPTER 3: EXPERIMENTATION

Introduction

The ability to establish and manipulate the direction of lipid mediator gradients poses a promising new approach in therapeutic angiogenesis and regenerative medicine. The purpose of this study is to evaluate how the direction of S1PR-targetted drug gradients and receptor subtype activation alter endothelial sprout morphology using a microfluidic device. To that end, we show that distal S1P1/3 stimulation promotes sprout formation and inhibits single-cell migration in endothelial cells whereas proximal stimulation does not. We also demonstrate that S1P3 subtype activation 1) is required for VEGF-induced sprouting both *in vitro* and *ex vivo*, 2) plays a significant role in regulating VE-cadherin expression *in vitro* and 3) promotes endothelial branching under flow *in vitro* and *in vivo*.

AIM 1: Determine the effects of S1P receptor agonist gradient directionality on endothelial sprout morphology in a microfluidic device

Device characterization and diffusion of S1P receptor-targeted drugs

The microfluidic device used allows for control over distal and proximal concentration gradients, as well as the ability to observe multiple observation regions within a single device (Fig. 1A). For all studies, cells were seeded into only one side of the device, and allowed to attach to the gel region before growth factors were introduced. In order to study the effects of gradient directionality on endothelial cell fate, S1PR agonist was either replenished in the cell channel (i.e. proximally, Fig. 1B[top]) or in the opposite channel (i.e. distally, Fig. 1B[bottom]). When included in a study, VEGF was

always replenished in the opposite channel. In order to evaluate the diffusion profile of S1PR agonist across the gel region, COMSOL computational software was used (Fig. 1C-D). Under static conditions, the concentration gradient at the cell barrier is maintained at 0.93 ± 0.05 mol/m^4 (mean$\pm$SEM) for the first 12 hours after changing media, and by hour 12 has dropped only 7.0% from the mean (Fig. 1C). Based on this, media in both channels was changed every 12 hours to maintain concentration gradients under static conditions. As expected under flow, the concentration gradient reaches and maintains a nearly linear diffusive profile ($R^2 \sim 0.95$) within 12 hours of initiating flow (Fig. 1D). Note that VEGF diffusion in this microfluidic device was previously modeled by Farahat et al.[57] Together, this model shows that concentration gradients can be established and maintained within acceptable ranges in the microfluidic device.

Distal S1P1/3 stimulation promotes arterial and venular sprout formation

We first investigated how proximal S1P1/3 stimulation (Fig. 2A) via FTY720 on arterial (HAAEC) and venular (HUVEC) endothelial cells affects the number of sprouts formed per imaging region (Fig. 2B). We observed no significant difference in the number of arterial or venular sprouts under proximal FTY720 stimulation compared to basal media (containing 5 ng/mL VEGF but no gradient of VEGF). In contrast, both HAAECs and HUVECs under distal S1P1/3 activation (Fig. 3A) displayed significantly greater number of sprouts (3.00 ± 0.33 and 2.39 ± 0.33 fold change, respectively) than those in basal media (Fig. 3B). Note that this increase in sprout density was observed even in the absence of VEGF.

Discussion

In the regulation of angiogenesis, not only is the absolute concentration of a signaling biomolecule important, but also the direction of its gradient with respect to blood vessels and the surrounding tissue.[60,61,62] To study the effect of sphingolipid gradient on endothelial sprouting, we used a parallel-channel microfluidic device in which the channels are analogous to pre-existing blood vessels and the central collagen gel represents tissue. This technique allows us to study how S1P signaling affects capillary formation in the absence of 1) biochemical cues that would otherwise be present in the blood and 2) interactions with immune and support cell types. Although proximal S1P1/3 stimulation caused no increase in sprout density, distal S1P1/3 stimulation in all studies promoted sprout formation. The effectiveness of a distal S1P gradient to induce sprouting has also been shown by Farahat et al., who used a microfluidic device seeded with human microvascular endothelial cells to demonstrate that S1P amplifies VEGF-induced sprouting.[57] Our data suggest that the high concentration of S1P found in the bloodstream under normal physiological conditions may serve to prevent unnecessary sprouting. Indeed, if proximal S1P receptor activation induced angiogenesis, one would expect hypersprouting to occur throughout the body, significantly altering cardiovascular stability and perfusion. It is also important to note that distal stimulation of FTY720 significantly enhanced sprout growth in the absence of VEGF, which suggests S1P1/3 targeting drug therapies may induce angiogenesis while avoiding possible side effects of VEGF administration.[63]

AIM 2: Evaluate the effects of a distal S1P1/3 targeted gradient on promoting arterial angiogenesis

The ability to deliver oxygen and nutrients to ischemic tissue or tissue-engineered constructs is crucial in developing novel strategies for therapeutic angiogenesis.[6-14,64-67] To that end, we focused our efforts on studying how S1P1/3 stimulation affects arterial sprouting in a microfluidic device. Based on our finding that a distal sphingolipid gradient is required to induce sprouting, the following studies include distal S1P1/3 activation. In addition, the combination of S1PR-targeted agonists and known angiogenic drugs such as VEGF may provide increased capillary morphogenesis, and hold even greater promise for translating this technology to the clinic. However, VEGF is also known to disrupt monolayer stability and induce endothelial migration.[68-70] Therefore, we normalized the following sprout density data to the number of migrating cells per group in order to evaluate endothelial barrier stability. A migrating cell was defined as an individual cell that has moved into the gel region and is not attached to the cell boundary or existing sprouts.

Distal S1P1/3 stimulation directs endothelial cell fate towards sprout formation, not migration

Under a distal S1PR agonist gradient (Fig. 4A), both VEGF and FTY720 + VEGF stimulation promoted significantly greater number of sprouts (3.75±0.43 and 5.48±0.52 fold change, respectively) in arterial cells than basal media (Fig. 4B). Notably, although not significant, FTY720 + VEGF induced a 46.01% increase in sprout density compared to VEGF. In agreement with our hypothesis, S1P1/3 stimulation in the presence of VEGF

promoted the greatest sprout-to-migration ratio (5.41±0.51) compared to VEGF alone (2.10±0.24) and basal media (1.00±0.30) (Fig. 4C). Together, these data suggest that distal S1P1/3 stimulation promotes endothelial sprout formation while inhibiting single-cell migration away from the endothelial barrier.

Distal S1P1/3 activation under flow promotes developed vasculature

Because arterial blood flow supplies tissue with oxygen and nutrients needed for survival and growth, we sought to investigate the effects of 1 µL/min flow on arterial capillary formation within the microfluidic device (Fig. 5A). Under flow, VEGF + FTY720 stimulation significantly enhanced sprout formation in HAAECs (6.83±0.43) compared to VEGF alone (4.61±0.35) and basal media (4.09±0.41) (Fig. 5B, values normalized to static basal media, bar not shown). Note that flow induced higher sprout formation in all groups than in the static basal media group, which agrees with findings in literature.[71] We also show that S1P1/3 stimulation, even in the presence of VEGF, significantly increased the ratio of sprouts-to-migrating cells (8.70±0.55) compared to VEGF alone (0.61±0.05) and basal media (1.00± 0.10) (Fig. 5C).

Discussion

We have shown using a microfluidic device that a distal S1P1/3-targeted drug delivery system increases arterial sprouting in the presence of VEGF. Not only are these newly-formed sprouts developed with greater frequency, but S1P1/3 stimulation also appears to stabilize the endothelial barrier by inhibiting migratory cell fate. Notably, the microfluidic data under flow reinforces our hypothesis that S1P1/3 stimulation promotes

and stabilizes sprout formation. In fact, under flow, FTY720 + VEGF treatment induces

significantly more sprouts than VEGF alone, even to a greater extent than under static

conditions. S1P1/3 stimulation under flow also produced the greatest sprout-to-migration

ratio in the presence of VEGF compared to VEGF alone, suggesting that even under flow

the sprouts formed in response to a distal FTY720 + VEGF gradient remain more stable

than those under only a VEGF gradient.

AIM 3: Determine the importance of S1P receptor subtype activation on endothelial sprouting and barrier stability

Select S1PR subtype activation is critical in developing effective angiogenic

therapies due to the diverse downstream signaling effects of these receptors.[25] Based on

our findings that distal S1P1/3 stimulation promotes sprout formation in arterial and

venular endothelial cells, we sought to investigate the relative importance of S1P1 and

S1P3 on 1) VEGF-induced sprouting, 2) VE-cadherin expression and 3) vascular

branching. An aortic ring assay was used to determine how endothelial responses to

S1PR subtype activation in the microfluidic device translated to a murine *ex vivo* model.

After observing that S1P1/3 stimulation inhibits endothelial migration, we decided to

further evaluate barrier permeability by selecting the adherens junction protein VE-

cadherin, which is largely responsible for homophilic interendothelial binding[72-74] and is

regulated by S1P1 and S1P3 signaling.[47,49] Lastly, we used a murine dorsal skinfold

window chamber model to evaluate the translatability of our microfluidic findings to an

in vivo vascular system.

Proximal S1P3 antagonism inhibits VEGF-induced sprouting

We first investigated the effect of proximal S1PR agonist stimulation in the presence of VEGF (Fig. 6A). As expected, VEGF induced a significantly greater sprout density in both arterial (1.84±0.20 fold change) and venular (2.0±0.17 fold change) cells compared to basal media, and was not significantly different from the number of spouts formed in the FTY720 + VEGF group (Fig. 6B). Notably, for both HAAECs and HUVECs, proximal S1P3 antagonism via VPC01091 significantly reduced VEGF-induced sprouting by 46.91% and 45.31%, respectively. To determine the translatability of this finding to a murine model, we performed an aortic ring assay. After 7 days *ex vivo*, we observed that VEGF stimulation promoted greater sprout formation from aortic rings in wild type mice than in those without VEGF (Fig. 6D). This sprouting was noticeably reduced in S1P3$^{-/-}$ mice. Together, these results demonstrate that S1P3 activity is required for endothelial sprout formation in the presence of VEGF.

Distal S1P3 activation is required to increase sprout stability

We then investigated how a distal gradient of S1PR-targeted drugs (Fig. 7A) impact surface protein expression. 6 days after seeding endothelial cells in the microfluidic devices, we performed immunofluorescent staining for VE-cadherin and quantified the total protein expression in the cell boundary and in the sprouts separately using ImageJ. Our findings agree with literature in that VE-cadherin expression is consistently reduced (-17.83±11.92% and -19.31±16.22%) under VEGF stimulation compared to basal media within arterial and venular cell boundaries, respectively (Fig. 7B-C, basal media has value of unity, bar not shown). Notably, for both HAAECs and

HUVECs, distal S1P1/3 stimulation in the presence of VEGF significantly increased the expression of VE-cadherin in both the cell boundary (4.57±0.64 and 2.29±0.35 A.U., respectively) and in the sprouts (1.82±0.18 and 1.45±0.24 A.U., respectively) compared to VEGF alone (0.82±0.12 and 0.81±0.16 for boundaries, 0.97±0.12 and 0.51±0.12 for sprouts, A.U.). For both arterial and venular sprouts, as well as for the venular boundary, FTY720 stimulation significantly increased VE-cadherin expression compared VPC01091 stimulation (1.82±0.18 vs. 0.95±0.10, 1.45±0.24 vs. 0.55±0.08, 2.29±0.35 vs. 0.87±0.18 A.U., respectively). Although not significant, FTY720 did promote a 95.99% increase in VE-cadherin expression compared to VPC01091 in the cell boundary for arterial cells. Together, these results demonstrate that S1P3 stimulation significantly increases VE-cadherin expression throughout the endothelial barrier and sprouts for both arterial and venular cells, even in the presence of VEGF.

Distal S1P3 activation increases vessel branching in vivo

As a final metric, we quantified the number of branch points between FTY720 and VPC01091 stimulation in the microfluidic device (Fig. 8A). Distal S1P1/3 stimulation was found to promote a significantly greater degree of branching in arterial cells than S1P1 agonism/S1P3 antagonism (2.92±0.52 vs. 1.57±0.35 branches, normalized to basal media). To compare these *in vitro* findings under flow to a physiological environment, we used a murine dorsal skinfold window chamber model (Fig. 8B-C). After normalizing the number of branch points 3 days post-implantation to that on day 0, the *in vivo* data demonstrate that FTY720 stimulation produced a significantly greater number of sprout branches (3.209±0.69) than did VPC01091

23

(1.00±0.14), in agreement with our microfluidic observations. Together, these results support our hypothesis that S1P3 stimulation is required to promote the most developed vasculature both in a microfluidic device under flow and within an *in vivo* mouse model.

Discussion

For applications that require VEGF, our data suggest that certain S1P receptors must also be functional. We first showed that S1P3 antagonism inhibits VEGF-induced sprouting in a microfluidic device (Fig. 6). The proximal gradient of S1P receptor-targeted drug (i.e. high concentration of VPC01091 in the cell channel) was chosen in order to maximally block S1P3, without the decrease in concentration the cells would have experienced had a distal gradient been used. Indeed, the dependence of VEGF-induced sprouting on S1P3 was confirmed *ex vivo* using an aortic ring assay in which S1P3$^{-/-}$ aortic cross sections showed noticeably less sprouting under VEGF stimulation than wild type mice. Others have studied the possibility of crosstalk between VEGF and S1P or S1PR-targeted drugs.[34,75,76] Licht et al. demonstrated that S1P3 subtype activation via KRX-725 potentiated VEGF-induced angiogenesis from *ex vivo* aortic rings.[76] Similarly, Lee et al. were not only able to show that S1P administration enhanced VEGF-induced sprouting, but also that antisense phophothioate oligonucleotide of S1P1 and S1P3 suppressed mature sprout formation *in vivo*.[34] Although our data agree with findings in literature, further studies need to be done to elucidate the exact mechanisms of crosstalk between VEGF and S1P signaling with regards to angiogenesis.

It is understood that VEGF induces sprouting from pre-existing vasculature;[39,61,77,78] however, the stability of those newly-formed vessels may be just as

24

important as sprout growth for regenerative medicine applications.[79-81] Here we have shown that VE-cadherin expression in both arterial and venular cells is S1PR-specific. VE-cadherin analysis was done on groups where VEGF was present because VEGF has been shown to increase barrier permeability by destabilizing VE-cadherin junctions.[36] For both the boundary and the sprouts, S1P1 agonism/S1P3 antagonism did not increase VE-cadherin expression for either cell type, suggesting that S1P3 activation is more important to VE-cadherin upregulation than S1P1 stimulation. This difference in downstream protein expression is plausible because S1P1 and S1P3 have independent signaling cascades that lead to VE-cadherin regulation.[49] It is important to note that S1P3 stimulation does not merely negate the VEGF-induced decrease in VE-cadherin expression, but significantly upregulates interendothelial junctions in both the cell boundary and the sprouts. Interestingly, S1P3-induced VE-cadherin expression in the cell boundary would be expected to decrease barrier permeability (thereby decreasing sprout formation), but the data suggest that S1P3 stimulation instead reduces the tendency of cells to migrate away from the cell boundary, even under a VEGF gradient. VE-cadherin junctions were upregulated in the sprouts as well, suggesting that S1P3 activation in the presence of VEGF creates more stable sprouts than VEGF alone or basal media. Notably, attenuation of endothelial migration did not suppress capillary morphogenesis, as distal S1P1/3 stimulation in the presence of VEGF was still found to increase sprout formation. Thus, distal stimulation of S1P3 targeted drugs and VEGF may provide the right balance of increased sprout formation, enhanced barrier stability, and inhibition of migratory cell fate.

One limitation of microfluidic devices is that, although they provide a high level of temporal and spatial control over the microenvironment, the results of these systems may not translate well to tissue responses *in vivo*. To address this concern, we compared our microfluidic findings with a murine dorsal skinfold window chamber analysis. Our *in vivo* results confirm that S1P3 functionality is important for achieving maximal sprout branching. Sefcik et al. were also able to demonstrate that S1P3 stimulation is critical for increasing vascular branching in the dorsal skinfold window chamber model.[52] Based on these findings, we expect a distal S1P3 agonistic delivery system that promotes a high degree of sprout formation while inhibiting individual cell migration to most effectively deliver oxygen and nutrients to surrounding tissue, and thus be a promising strategy in therapeutic angiogenesis.

FUTURE DIRECTIONS

It is important to note that the microfluidic results observed here are specific to the concentration of solutes chosen and geometry of the device used. Das et al. tested the effects of VEGF between 10 – 40 ng/mL on endothelial cell sprouting in a microfluidic device and found that 40 ng/mL VEGF induced the longest and most frequent sprout formation.[56] We chose to use 250 nM S1PR-targeted drugs because S1P concentrations in the blood vary between 200 – 500 nM.[82] Using different concentrations of VEGF and S1PR-targeted drugs would be expected to impact the balance between migration and capillary morphogenesis. If the concentration of VEGF were significantly increased, we would expect an increase in endothelial wall and sprout permeability, increasing the probability that individual cells will transition from a sprouting to migratory cell fate. In

addition, overstimulation of S1P3 may induce VE-cadherin junctions beyond that which is allowable for sprout formation. Although further studies are needed to optimize the microfluidic system for different concentrations of S1PR agonist, our data suggests that, within the microfluidic geometry used, distal 250 nM S1P1/3 agonism in the presence of 40 ng/mL VEGF strikes a favorable balance of increased capillary morphogenesis while stabilizing the monolayer and newly-formed sprouts.

Furthermore, the findings outlined in this study may lay the platform for more complex, co-culture analysis of endothelial behavior under S1PR-targeted drugs. Co-culture microfluidic systems maintain tight control over temporal and spatial cues while adding a level of complexity that may be closer to *in vivo* physiology. Chung et al. demonstrated that endothelial cells co-cultured with either cancer lines or smooth muscle cells elicited different capillary formation responses.[83] MTLn3 cancer cells had a pro-angiogenic effect on endothelial cells, whereas the U87MG cancer cell line produced a minimal response and 10T ½ smooth muscle cells suppressed sprouting. Zheng et al. demonstrated that, upon injection of whole blood into a microfluidic device pre-seeded with a monolayer of endothelial cells, they could mimic both healthy and thrombotic physiological states through brief stimulation of the inflammatory agent phorbol-12-myristate-13-acetate (PMA).[84] Upon PMA exposure, platelet aggregates immediately began to form on the endothelial surface, and after 1 hour of blood perfusion, leukocytes were observed to attach and migrate through the endothelial wall into the surrounding gel. However, it is important to note that Zheng's *in vitro* blood vessels were formed from endothelial cell attachment and monolayer formation, not neovascularization. Thus, it would be interesting to co-culture arterial and venular cells under VEGF and S1PR

27

agonist gradients in order to create an *in vitro* capillary bed where interstitial fluid and solute exchange could be studied within a microfluidic platform like the one outlined here.

CONCLUSION

We have shown that the gradient direction of S1PR-targeted drugs is critical for eliciting an angiogenic response from endothelial cells. Distal S1P3 activation was shown to be necessary for improved sprout formation, stabilization and branching even in the absence of endocrine or mural cues. Together, these data suggest that S1P gradient and receptor subtype activation are important criteria to consider when developing novel angiogenic therapies.
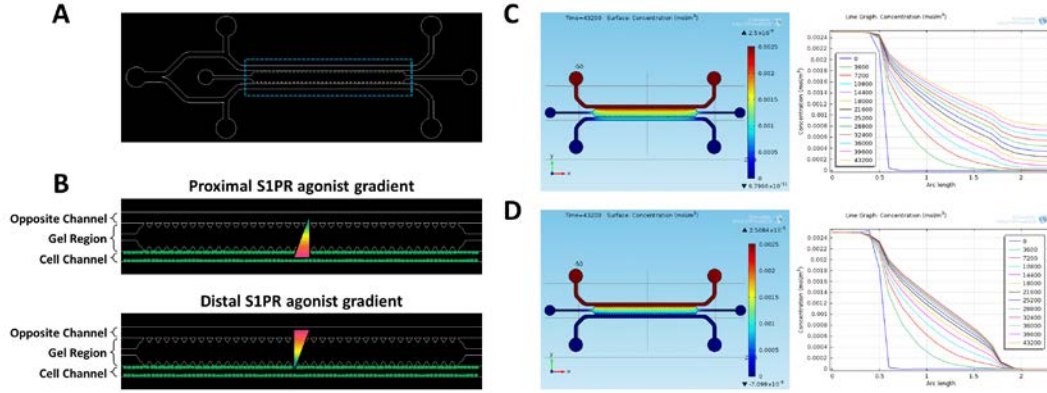
Figure 1. Experimental setup and S1PR agonist diffusion model. A) Microfluidic

device. B) Schematic of outlined area in (A), showing proximal (top) and distal (bottom)

S1P receptor agonist gradients (Red = high concentration. Blue = low concentration.

Green ovals = cells). C) Computational model of static S1PR agonist diffusion profile at

12 hr (left) and concentration vs. distance plot (right) for t = 0 to t = 12 hr. D) Diffusion

profile of S1PR agonist at 12 hr (left) and concentration vs. distance plot (right) for t = 0

to t = 12 hr under 1 µL/min flow.
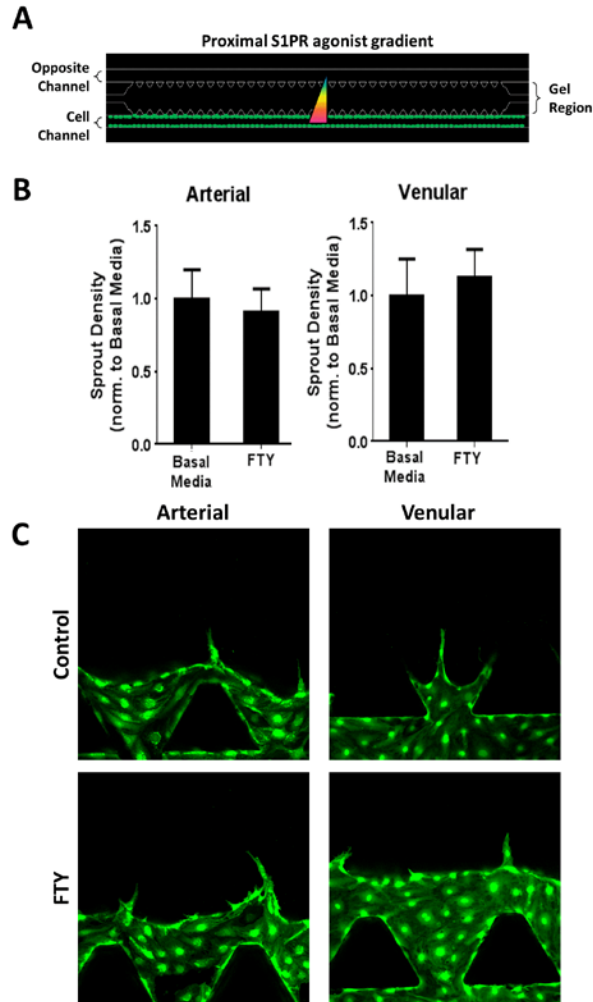
Figure 2. Proximal agonist stimulation of S1P1/3 does not induce sprouting. A) Schematic of proximal S1PR agonist stimulation in the absence of VEGF. B) Sprout density, normalized to basal media control, for HAAECs (left) and HUVECs (right). C) Representative images of (B). Magnification = 20x. FTY = FTY720. Error bars represent standard error. *, P < 0.05.
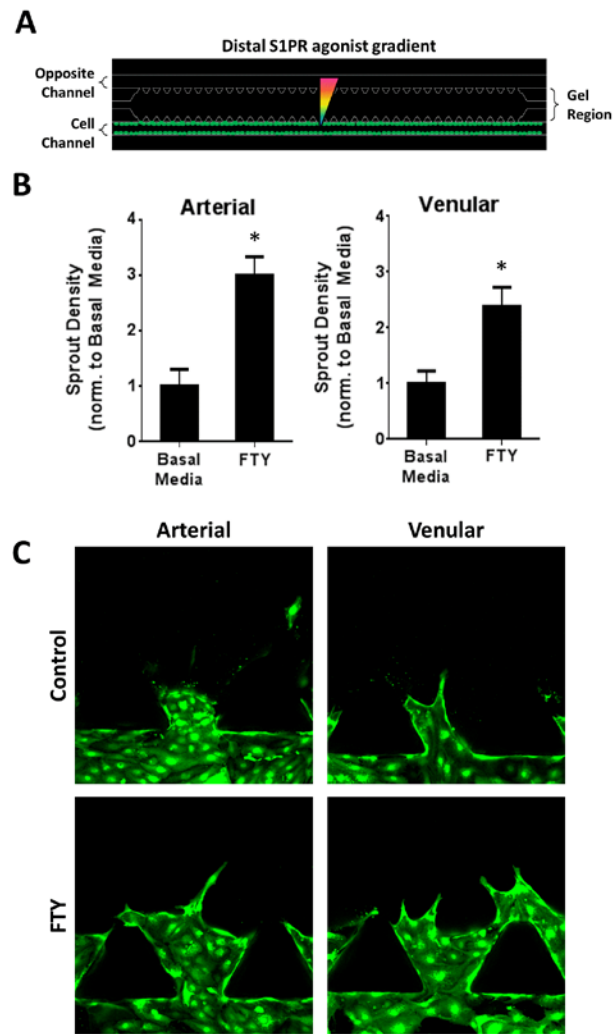
Figure 3. Distal S1P1/3 stimulation promotes sprout formation in arterial and venular endothelial cells. A) Schematic of distal S1PR agonist stimulation in the absence of VEGF. B) Sprout density of HAAECs and HUVECs under distal S1PR agonist stimulation, normalized to basal media. C) Representative images of (B). Magnification = 20x. Error bars represent standard error. *, P < 0.05.
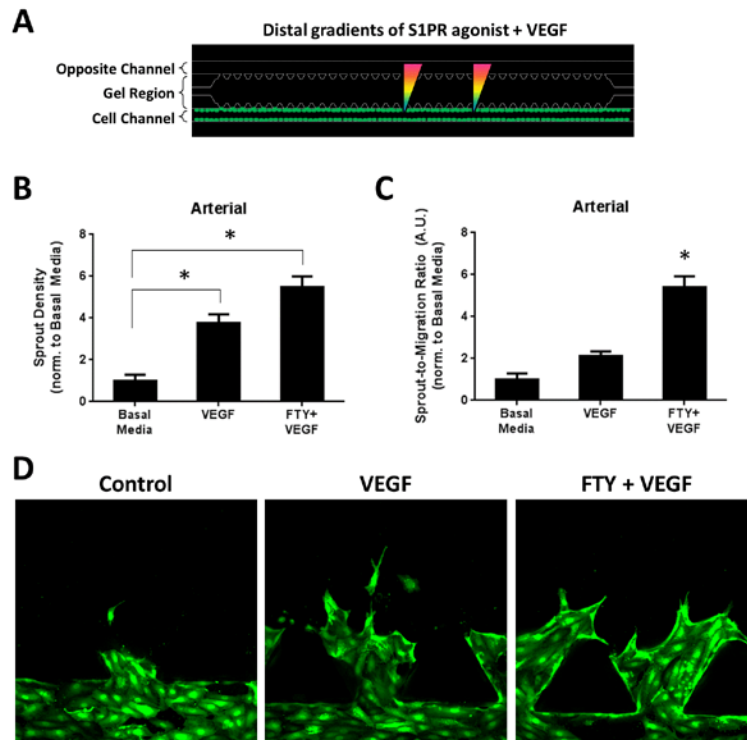
Figure 4. Distal S1P1/3 stimulation promotes and stabilizes sprouting in arterial endothelial cells. A) Schematic of static distal S1PR agonist stimulation in the presence of VEGF. B) Sprout density of HAAECs normalized to basal media under distal agonist stimulation. C) Sprout-to-migration ratio (A.U.) for HAAECs, normalized to basal media. D) Representative images of sprouting and migrating cell data shown in (B) and (C). Magnification = 20x. Error bars represent standard error. *, P < 0.05.
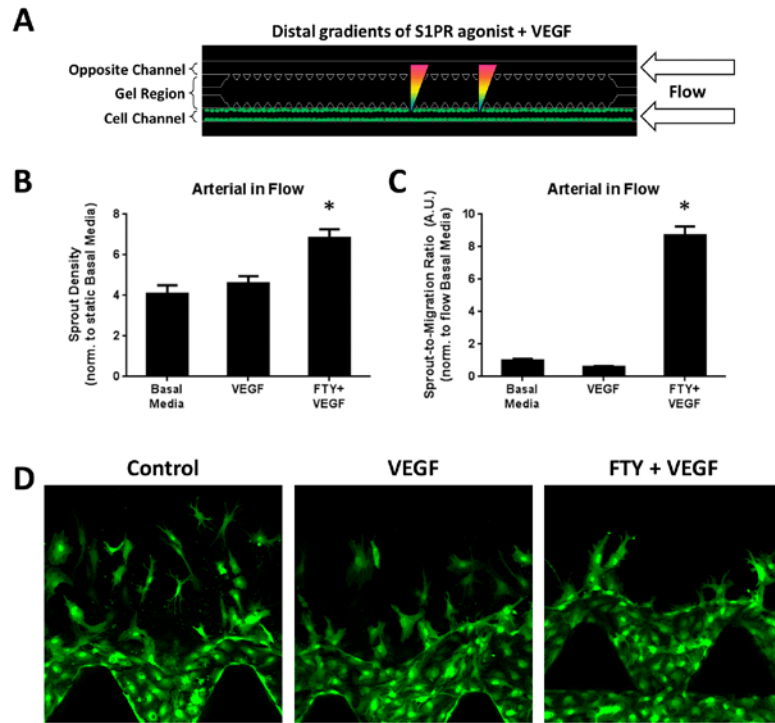
Figure 5. Distal S1P1/3 stimulation under flow promotes stable arterial sprout formation. A) Schematic of distal S1PR agonist stimulation in the presence of VEGF and flow. B) Sprout density for HAAECs under flow, normalized to static basal media (value of unity, bar not shown). C) Sprout-to-migration ratio (A.U.) for HAAECs under flow, normalized to flow basal media. D) Representative images of sprouting and migration data shown in (B) and (C). Magnification = 20x. Error bars represent standard error. *, $P < 0.05$.
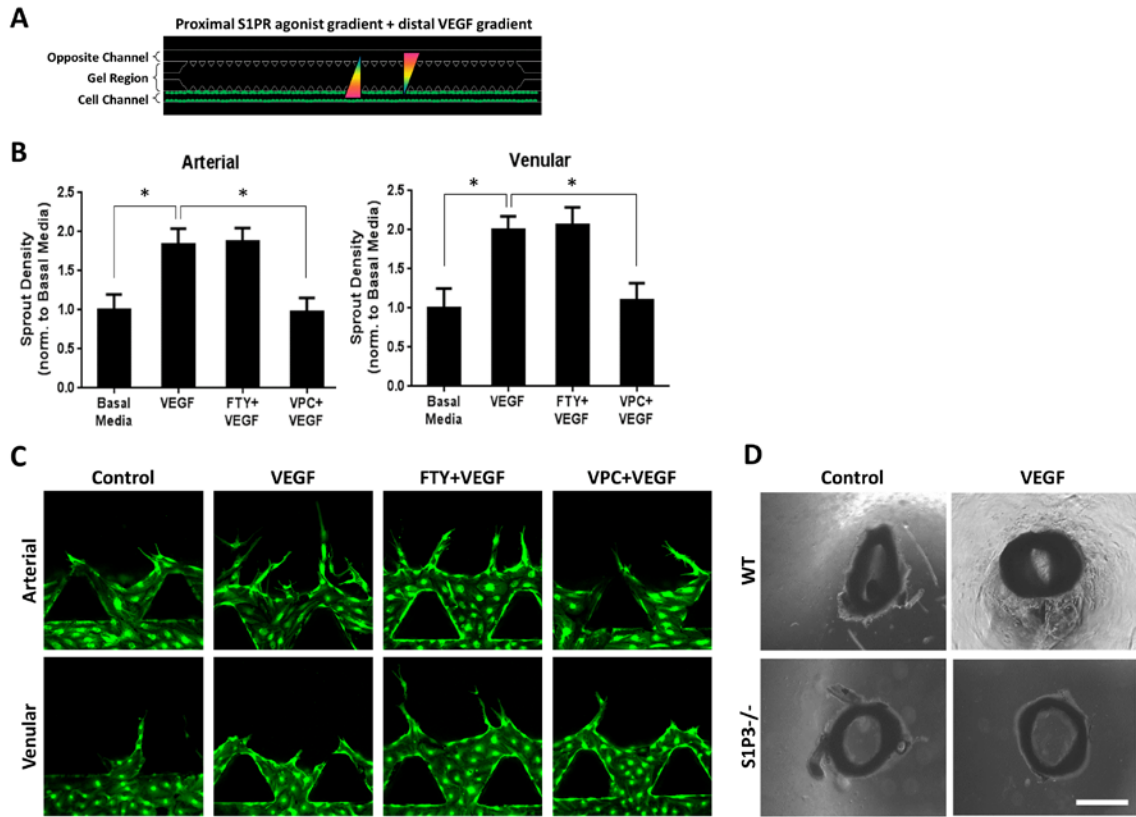
Figure 6. Proximal agonist stimulation of S1P3 inhibitors decreases VEGF-induced endothelial sprouting. A) Schematic of proximal stimulation in the presence of VEGF. B) Sprout density for HAAECs and HUVECs in the presence of VEGF, normalized to basal media. C) Representative images of sprout density shown in (B). Magnification = 20x. D) Representative phase contrast images of *ex vivo* aortic ring assay. Scale bar = 1 mm. VPC = VPC01091. WT = wild type. Error bars represent standard error. *, P < 0.05.
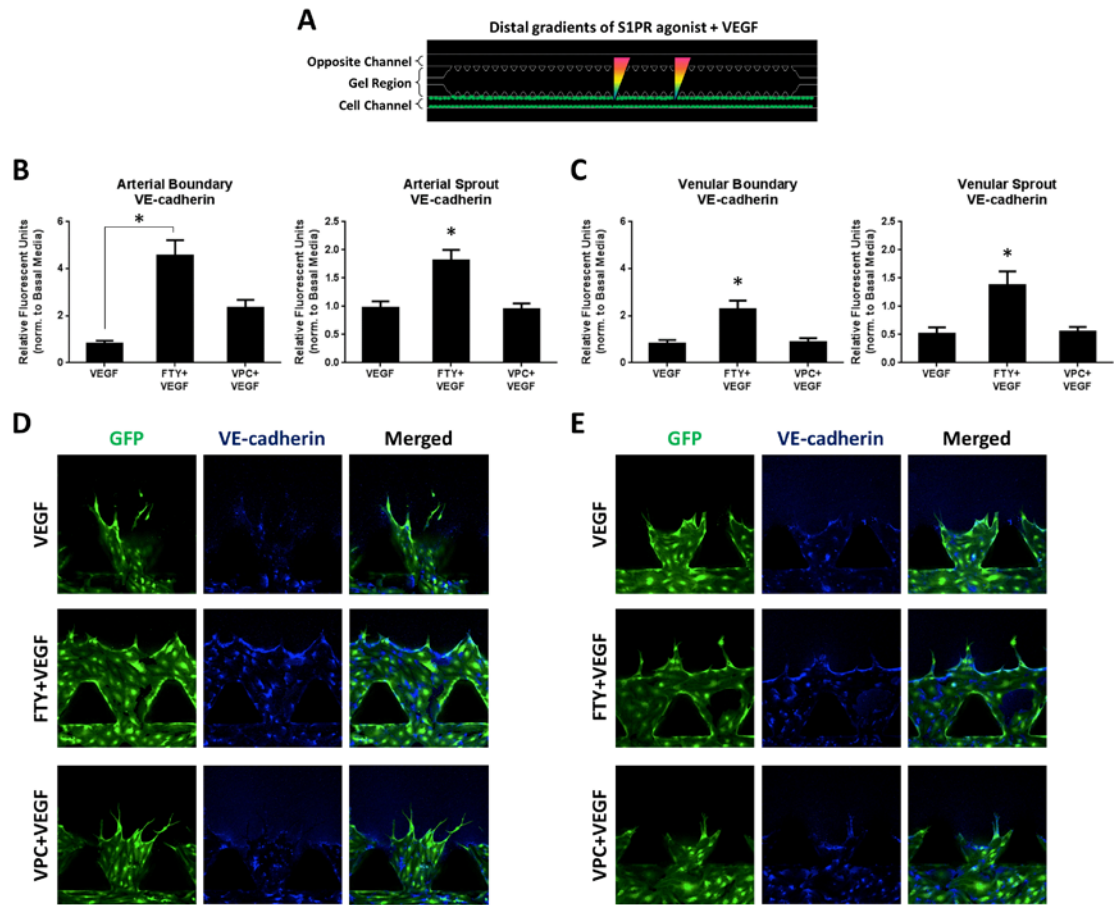
Figure 7. Distal S1P1/3 stimulation stabilizes vasculature via VE-cadherin. A) Schematic of static distal S1PR agonist stimulation in the presence of VEGF. B) VE-cadherin expression (relative fluorescent units, RFU) in the arterial cell boundary (left) and sprouts (right) per region, normalized to basal media (value of unity, bar not shown). C) VE-cadherin expression (RFU) in the venular cell boundary (left) and sprouts (right) per region, normalized to basal media (value of unity, bar not shown). D-E) Representative images showing GFP and VE-cadherin channels, as well as merged images for HAAECs (D) and HUVECs (E). Magnification = 20x. Error bars represent standard error. *, $P < 0.05$.
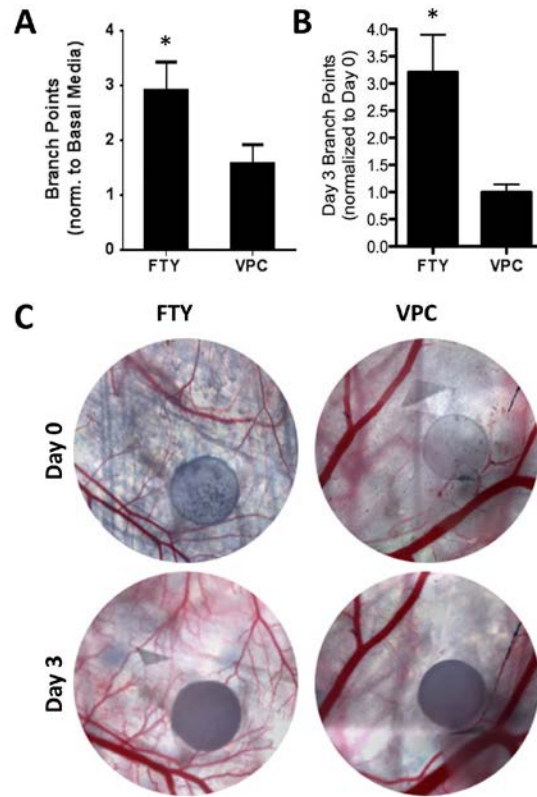
Figure 8. Distal S1P1/3 stimulation under flow promotes vessel branching. A)
Number of branch points of arterial endothelial cells under distal S1PR agonist
stimulation and flow in the microfluidic device, normalized to basal media (value of
unity, bar not shown). B) Change in number of branch points within a dorsal skinfold
window chamber model between 0 and 3 days post implantation. C) Representative
images of (B) under FTY720 or VPC01091 stimulation. Circular film diameter = 1 mm.
Error bars represent standard error. *, $P < 0.05$.

APPENDIX II: ACKNOWLEDGEMENTS

APPENDIX III: REFERENCES

1. Weidner N, Folkman J, Pozza F, Bevilacqua P, Allred EN, Moore DH, Meli S, and Gasparini G. Tumor angiogenesis: a new significant and independent prognostic indicator in early-stage breast carcinoma. J Natl Cancer Inst **84**, 1875, 1992.

2. Carmeliet, P. Mechanisms of angiogenesis and arteriogenesis. Nat Med **6**, 389, 2000.

3. Ferrara, N., and Kerbel, R.S. Angiogenesis as a therapeutic target. Nature **438**, 967, 2005.

4. Kerbel, R.S. Tumor angiogenesis. N Engl J Med **358**, 2039, 2008.

5. Oh, W.K., McDermott, D., Porta, C., Levy, A., Elaidi, R., Scotte, F., Hawkins, R., Castellano, D., Bellmunt, J., Rha, S.Y., Sun, J.M., Nathan, P., Feinberg, B.A., Scott, J., McDermott, R., Ahn, J.H., Wagstaff, J., Chang, Y.H., Ou, Y.C., Donnellan, P., Huang, C.Y., McCaffrey, J., Chiang, P.H., Chuang, C.K., Korves, C., Neary, M.P., Diaz, J.R., Mehmud, F., and Duh, M.S. Angiogenesis inhibitor therapies for advanced renal cell carcinoma: Toxicity and treatment patterns in clinical practice from a global medical chart review. Int J Oncol **44**, 5, 2014.

6. Isner, J.M., Walsh, K., Symes, J., Pieczek, A., Takeshita, S., Lowry, J., Rossow, S., Rosenfield, K., Weir, L., Brogi, E., and Schainfeld, R. Arterial gene therapy for therapeutic angiogenesis in patients with peripheral artery disease. Circulation **91**, 2687, 1995.

7. Collinson, D.J., and Donnelly, R. Therapeutic angiogenesis in peripheral artery disease: can biotechnology produce an effective collateral circulation? Eur J Vasc Endovasc Surg **28**, 9, 2004.

8. Troidl, K., and Schaper, W. Arteriogenesis versus angiogenesis in peripheral artery disease. Diabetes Metab Res Rev **28**, 27, 2012.

9. Grochot-Przeczek, A., Dulak, J., and Jozkowicz, A. Therapeutic angiogenesis for revascularization in peripheral artery disease. Gene **525**, 222, 2013.

10. Frangogiannis, N.G. Stromal cell-derived factor-1-mediated angiogenesis for peripheral arterial disease. Circulation **123**, 1267, 2011.

11. Krupinski, J., Kaluza, J., Kumar, P., Kumar, S., and Wang, J.M. Role of angiogenesis in patients with cerebral ischemic stroke. Stroke **25**, 1794, 1994.

12. Wei, L., Keogh, C.L., Whitaker, V.R., Theus, M.H., and Yu, S.P. Angiogenesis and stem cell transplantation as potential treatments of cerebral ischemic stroke. Pathophysiology **12**, 47, 2005.

13. Arenillas, J.F., Sobrino, T., Castillo, J., and Dávalos, A. The role of angiogenesis in damage and recovery from ischemic stroke. Curr Treat Options Cardivasc Med **9**, 205, 2007.

14. Font, M.A., Arboix, A., and Krupinski, J. Angiogenesis, Neurogenesis and Neuroplasticity in Ischemic Stroke. Curr Cardiol Rev **6**, 238, 2010.

15. Roberts, A.B., Sporn, M.B., Assoian, R.K., Smith, J.M., Roche, N.S., Wakefield, L.M., Heine, U.I., Liotta, L.A., Falanga, V., and Kehri, J.H. Transforming growth factor type beta: rapid induction of fibrosis and angiogenesis in vivo and stimulation of collagen formation in vitro. Proc Natl Acad Sci U S A **83**, 4167, 1986.

16. Folkman, J., and Klagsbrun, M. Angiogenic factors. Science **235**, 442, 1987.

17. Ferrara, N., and Alitalo, Kari. Clinical applications of angiogenic growth factors and their inhibitors. Nat Med **5**, 1359, 1999.

18. Yancopoulos, G.D., Davis, S., Gale, N.W., Rudge, J.S., Wiegand, S.J., and Holash, J. Vascular-specific growth factors and blood vessel formation. Nature **407**, 242, 2000.

19. John, A., and Tuszynski, G. The role of matrix metalloproteinases in tumor angiogenesis and tumor metastasis. Pathol Oncol Res **7**, 14, 2001.

20. Rundhaug, J.E. Matrix metalloproteinases and angiogenesis. J Cell Mol Med **9**, 267, 2005.

21. Belperio, J.A., Keane, M.P., Arenberg, D.A., Addison, C.L., Ehlert, J.E., Burdick, M.D., and Strieter, R.M. CXC chemokines in angiogenesis. J Leukoc Biol **68**, 1, 2000.

22. Salcedo, R., and Oppenheim, J.J. Role of chemokines in angiogenesis: CXCL12/SDF-1 and CXCR4 interaction, a key regulator of endothelial cell responses. Microcirculation **10**, 359, 2003.

23. Fierro, I.M., Kutok, J.L., and Serham, C.N. Novel lipid mediator regulators of endothelial cell proliferation and migration: Aspirin-triggered-15R-lipoxin A_4 and Lipoxin A_4. J Parmacol Exp Ther **300**, 385, 2002.

24. Ogretmen, B., and Hannun, Y.A. Biologically active sphingolipids in cancer pathogenesis and treatment. Nat Rev Cancer **4**, 604, 2004.

25. Takuwa, Y., Du, W., Qi, X., Okamoto, Y., Takuwa, N., and Yoshioka, K. Roles of sphingosine-1-phosphate signaling in angiogenesis. World J Biol Chem **1**, 298, 2010.

26. Takabe, K., Paugh, S.W., Milstien, S., and Spiegel, S. "Inside-out" signaling of sphingosine-1-phosphate: Therapeutic targets. Pharmacol Rev **60**, 181, 2008.

27. Rosen, H., Gonzalez-Cabrera, P., Marsolais, D., Cahalan, S., Don, A.S., and Sanna, M.G. Modulating tone: the overture of S1P receptor immunotherapeutics. Immunol Rev **223**, 221, 2008.

28. Marsolais, D., and Rosen, H. Chemical modulators of sphingosine-1-phosphate receptors as barrier-oriented therapeutic molecules. Nat Rev Drug Discov **8**, 297, 2009.

29. Spiegel, S., and Milstien, S. The outs and the ins of sphingosine-1-phosphate in immunity. Nat Rev Immunol **11**, 403, 2011.

30. Strader, C.R., Pearce, C.J., and Oberlies, N.H. Fingolimod (FTY720): A recently approved multiple sclerosis drug based on a fungal secondary metabolite. J Nat Prod **74**, 900, 2011.

31. Awojoodu, A.O., Ogle, M.E., Sefcik, L.S., Bowers, D.T., Martin, K., Brayman, K.L., Lynch, K.R., Peirce-Cottler, S.M., and Botchwey, E. Sphingosine 1-phosphate receptor 3 regulates recruitment of anti-inflammatory monocytes to microvessels during implant arteriogenesis. Proc Natl Acad Sci U S A **110**, 13785, 2013.

32. Kono, M., Mi, Y., Liu, Y., Sasaki, T., Allende, M.L., Wu, Y., Yamashita, T., and Proia, R.L. The sphingosine-1-phosphate receptors S1P1, S1P2, and S1P3 function coordinately during embryonic angiogenesis. J Biol Chem **279**, 29367, 2004.

33. Lee, O.H., Kim, Y.M., Lee, Y.M., Moon, E.J., Lee, D.J., Kim, J.H., Kim, K.W., and Kwon, Y.G. Sphingosine 1-phosphate induces angiogenesis: its angiogenic action and

signaling mechanism in human umbilical vein endothelial cells. Biochem Biophys Res Commun **264**, 743, 1999.

34. Lee, M.J., Thangada, S., Claffey, K.P., Ancellin, N., Liu, C.H., Kluk, M., Sha'afi, R.I., and Hla, T. Vascular endothelial cell adherens junction assembly and morphogenesis induced by sphingosine-1-phosphate. Cell **99**, 301, 1999.

35. Liu, Y., Wada, R., Yamashita, T., Mi, Y., Deng, C.X., Hobson, J.P., Rosenfeldt, H.M., Nava, V.E., Chae, S.S., Lee, M.J., Liu, C.H., Hla, T., Spiegel, S., and Proia, R.L. Edg-1, the G protein-coupled receptor for sphingosine-1-phosphate, is essential for vascular maturation. J Clin Invest **106**, 951, 2000.

36. Esser, S., Lampugnani, M.G., Corada, M., Dejana, E., and Risau, W. Vascular endothelial growth factor induces VE-cadherin tyrosine phosphorylation in endothelial cells. J Cell Sci **111**, 1853, 1998.

37. Fleming, W.H., Endothelial cell-specific markers: Going… going… gone. Blood **106**, 769, 2005.

38. Hänel, P., Andréani, P., Gräler, M.H. Erythrocytes store and release sphingosine 1-phosphate in blood. FASEB J **21**, 1202, 2007.

39. Byrne, A.M., Bouchier-Hayes, D.J., and Harmey, J.H. Angio Angiogenic and cell survival functions of vascular endothelial growth factor (VEGF). J Cell Med **9**, 777, 2005.

40. Gavard, J. and Gutkind, J.S. VEGF controls endothelial-cell permeability by promoting the beta-arrestin-dependent endocytosis of VE-cadherin. Nat Cell Bio **8**, 1223, 2006.

41. Wang, S., Li, X., Parra, M., Verdin, E., Bassel-Duby, R., and Olson, E.N. Control of endothelial cell proliferation and migration by VEGF signaling to histone deacetylase 7. Proc Natl Acad Sci U S A **105**, 7738, 2008.

42. Nourse, M.B., Halpin, D.E., Scatena, M., Mortisen, D.J., Tulloch, N.L., Hauch, K.D., Torok-Storb, B., Ratner, B.D., Pabon, L., and Murry, C.E. VEGF induces differentiation of functional endothelium from human embryonic stem cells: implications for tissue engineering. Arterioscler Thromb Vasc Biol **30**, 80, 2010.

43. Lebman, D.A., and Spiegel, S. Cross-talk at the crossroads of sphingosine-1-phosphate, growth factors, and cytokine signaling. J Lipid Res **49**, 1388, 2008.

44. Pyne, N.J., and Pyne, S. Sphingosine 1-phosphate and cancer. Nat Rev Cancer **10**, 489, 2010.

45. Anderson, G., and Maes, M. Reconceptualizing Adult Neurogenesis: Role for Sphingosine-1-Phosphate and Fibroblast Growth Factor-1 in Co-ordinating Astrocyte-Neuronal Precursor Interactions. CNS Neurol Disord Drug Targets, Epub, 2013.

46. Gavrilovskaya, I.N., Gorbunova, E.E., Mackow, N.A., and Mackow, E.R. Hantaviruses direct endothelial cell permeability by sensitizing cells to vascular permeability factor VEGF, while angiopoietin 1 and sphingosine 1-phosphate inhibit hantavirus-directed permeability. J Virol **82**, 5797, 2008.

47. Gaengel, K., Niaudet, C., Hagikura, K., Laviña, B., Muhl, L., Hofmann, J.J., Ebarasi, L., Nyström, S., Rymo, S., Chen, L.L., Pang, M.F., Jin, Y., Raschperger, E., Roswall, P., Schulte, D., Benedito, R., Larsson, J., Hellström, M., Fuxe, J., Uhlén, P., Adams, R., Jakobsson, L., Majumdar, A., Vestweber, D., Uv, A., and Betsholtz, C. The sphingosine-1-phosphate receptor S1PR1 restricts sprouting angiogenesis by regulating the interplay between VE-cadherin and VEGFR2. Dev Cell **23**, 587, 2012.

48. Ngai, C.Y., and Yao, X. Vascular responses to shear stress: The involvement of mechanosensors in endothelial cells. Open Circ Vasc J **3**, 85, 2010.

49. Gaengel, K., Genové, G., Armulik, A., and Betsholtz, C. Endothelial-mural cell signaling in vascular development and angiogenesis. Aterioscler Thromb Vasc Biol **29**, Epub, 2009.

50. Anelli, V., Gault, C.R., Snider, A.J., and Obeid, L.M. Role of sphingosine kinase-1 in paracrine/transcellular angiogenesis and lymphangiogenesis in vitro. FASEB J **24**, 2727, 2010.

51. Wilkerson, B.A., Grass, G.D., Wing, S.B., Argraves, W.S., and Argraves, K.M. S1P carrier-dependent regulation of endothelial barrier: HDL-S1P prolongs endothelial barrier enhancement as compared to albumin-S1P via effects on levels, trafficking and signaling of S1P1. J Biol Chem **287**, 44645, 2012.

52. Sefcik, L.S., Aronin, C.E., Awojoodu, A.O., Shin, S.J., Mac Gabhann, F., MacDonald, T.L., Wamhoff, B.R., Lynch, K.R., Peirce, S.M., and Botchwey, E.A. Selective activation of sphingosine 1-phosphate receptors 1 and 3 promotes local microvascular network growth. Tissue Eng Part A **17**, 617, 2011.

53. Schaff, U.Y., Xing, M.M., Lin, K.K., Pan, N., Jeon, N.L., and Simon, S.I. Vascular mimetics based on microfluidics for imaging the leukocyte--endothelial inflammatory response. Lab Chip **7**, 448, 2007.

54. van der Meer, A.D., Orlova, V.V., ten Dijke, P., van den Berg, A., and Mummery, C.L. Three-dimensional co-cultures of human endothelial cells and embryonic stem cell-derived pericytes inside a microfluidic device. Lab Chip **13**, 3562, 2013.

55. Jeong, G.S., Kwon, G.H., Kang, A.R., Jung, B.Y., Park, Y., Chung, S., and Lee, S.H. Microfluidic assay of endothelial cell migration in 3D interpenetrating polymer semi-network HA-Collagen hydrogel. Biomed Microdevices **13**, 717, 2011.

56. Das, A. Lauffenburger, D., Asada, H., and Kamm, R. Determining cell fate transition probabilities to VEGF/Ang 1 levels: Relating computational modeling to microfluidic angiogenesis studies. Cell Mol Bioeng **3**, 345, 2010.

57. Farahat W.A., Wood, L.B., Zervantonakis, I.K., Schor, A., Ong, S., Neal, D., Kamm, R.D., and Asada, H.H. Ensemble analysis of angiogenic growth in three-dimensional microfluidic cell cultures. PLoS One **7**, e37333, 2012.

58. Vickerman, V., Blundo, J., Chung, S., and Kamm, R. Design, fabrication and implementation of a novel multi-parameter control microfluidic platform for three-dimensional cell culture and real-time imaging. Lab Chip **8**, 1468, 2008.

59. Das, A., Lauffenburger, D., Asada, H., and Kamm, R.D. A hybrid continuum-discrete modelling approach to predict and control angiogenesis: analysis of combinatorial growth factor and matrix effects on vessel-sprouting morphology. Phil Trans R Soc A **368**, 2937, 2010.

60. Knighton, D.R., Silver, I.A., and Hunt, T.K. Regulation of wound-healing angiogenesis-effect of oxygen gradients and inspired oxygen concentration. Surgery **90**, 262, 1981.

61. Gerhardt, H., Golding, M., Fruttiger, M., Ruhrberg, C., Lundkvist, A., Abramsson, A., Jeltsch, M., Mitchell, C., Alitalo, K., Shima, D., and Betsholtz, C. VEGF guides

angiogenic sprouting utilizing endothelial tip cell filopodia. J Cell Bio **161**, 1163, 2003.

62. Schipani, E., Wu, C., Rankin, E.B., and Giaccia, A.J. Regulation of bone marrow angiogenesis by osteoblasts during bone development and homeostasis. Front Endocrinol (Lausanne) **4**, Epub, 2013.

63. Eskens, F.A., Verweij, J. The clinical toxicity profile of vascular endothelial growth factor (VEGF) and vascular endothelial growth factor receptor (VEGR) targeting angiogenesis inhibitors; a review. Eur J Cancer **42**, 3127, 2006.

64. Bouhadir, K.M., and Mooney, D.J. Promoting angiogenesis in engineered tissues. J Drug Target **9**, 397, 2001.

65. Cassell, O.C., Hofer, S.O., Morrison, W.A., and Knight, K.R. Vascularisation of tissue-engineered grafts: the regulation of angiogenesis in reconstructive surgery and in disease states. Br J Plast Surg **55**, 603, 2002.

66. Laschke, M.W., Harder, Y., Amon, M., Martin, I., Farhadi, J., Ring, A., Torio-Padron, N., Scramm, R., Rücker, M., Junker, D., Häufel, J.M., Carvalho, C., Heberer, M., Germann, G., Vollmar, B., and Menger, M.D. Angiogenesis in tissue engineering: breathing life into constructed tissue substitutes. Tissue Eng **12**, 2093, 2006.

67. Jabbarzadeh, E., Starnes, T., Khan, Y.M., Jiang, T., Wirtel, A.J., Deng, M., Lv, Q., Nair, L.S., Doty, S.B., and Laurencin, C.T. Induction of angiogenesis in tissue-engineered scaffolds designed for bone repair: a combined gene therapy-cell transplantation approach. Proc Natl Acad Sci U S A **105**, 11099, 2008.

68. Yoshida, A., Anand-Apte, B., and Zetter, B.R. Differential endothelial migration and proliferation to basic fibroblast growth factor and vascular endothelial growth factor. Growth Factors **13**, 57, 1996.

69. Rousseau, S., Houle, F., Landry, J., and Huot, J. p38 MAP kinase activation by vascular endothelial growth factor mediates actin reorganization and cell migration in human endothelial cells. Oncogene **15**, 2169, 1997.

70. Neufeld, G., Cohen, T., Gengrinovitch, S., and Poltorak, Z. Vascular endothelial growth factor (VEGF) and its receptors. FASEB J **13**, 9, 1999.

71. Jung, B., Obinata, H., Galvani, S., Mendelson, K., Ding, B.S., Skoura, A., Kinzel, B., Brinkmann, V., Rafii, S., Evans, T., and Hla, T. Flow-regulated endothelial S1P receptor-1 signaling sustains vascular development. Dev Cell **23**, 600, 2012.

72. Lampugnani, M.G., Corada, M., Caveda, L., Breviario, F., Ayalon, O., Geiger, B., and Dejana, E. The molecular organization of endothelial cell to cell junctions: differential association of plakoglobin, beta-catenin, and alpha-catenin with vascular endothelial cadherin (VE-cadherin). J Cell Bio **129**, 203, 1995.

73. Vestweber, D. VE-cadherin: the major endothelial adhesion molecule controlling cellular junctions and blood vessel formation. Arterioscler Thromb Vasc Biol **28**, 223, 2008.

74. Dejana, E., Orsenigo, F., and Lampugnani, M.G. The role of adherens junctions and VE-cadherin in the control of vascular permeability. J Cell Sci **121**, 2115, 2008.

75. Carmeliet, P., and Jain, R.K. Molecular mechanisms and clinical applications of angiogenesis. Nature **473**, 298, 2011.

76. Licht, T., Tsirulnikov, L., Reuveni, H., Yarnitzky, T., and Ben-Sasson, S.A. Induction of pro-angiogenic signaling by a synthetic peptide derived from the second intracellular loop of S1P3 (EDG3). Blood **102**, 2099, 2003.

77. Grunewald, M., Avraham, I., Dor, Y., Bachar-Lustig, E., Itin, A., Jung, S., Chimenti, S., Landsman, L., Abramovitch, R., and Keshet, E. VEGF-induced adult neovascularization: recruitment, retention, and role of accessory cells. Cell **124**, 175, 2006.

78. Mancuso, M.R., Davis, R., Norberg, S.M., O'Brien, S., Sennino, B., Nakahara, T., Yao, V.J,. Inai, T., Brooks, P., Freimark, B., Shalinsky, D.R., Hu-Lowe, D.D., and McDonald, D.M. Rapid vascular regrowth in tumors after reversal of VEGF inhibition. J Clin Invest 116, 2610, 2006.

79. Cao, R., Bråkenhielm, E., Pawliuk, R., Wariaro, D., Post, M.J., Wahlberg, E., Leboulch, P., and Cao, Y. Angiogenic synergism, vascular stability and improvement of hind-limb ischemia by a combination of PDGF-BB and FGF-2. Nat Med **9**, 604, 2003.

80. Jain, R.K. Molecular regulation of vessel maturation. Nat Med **9**, 685, 2003.

81. Koike, N., Fukumura, D., Gralla, O., Au, P., Schechner, J.S., and Jain, R.K. Tissue engineering: creation of long-lasting blood vessels. Nature **428**, 138, 2004.

82. Schubert, R. Sphingosine-1-phosphate in the circulatory system: Cause and therapeutic target for vascular dysfunction? Cardiovasc Res **70**, 9, 2006.

83. Chung, S., Sudo, R., Mack, P.J., Wan, C.R., Vickerman, V., and Kamm, R.D. Cell migration into scaffolds under co-culture conditions in a microfluidic platform. Lab Chip **9**, 269, 2009.

84. Zheng, Y., Chen, J., Craven, M., Choi, N.W., Totorica, S., Diaz-Santana, A., Kermani, P., Hempstead, B., Fischbach-Teschl, C., López, J.A., and Stroock, A.D. In vitro microvessels for the study of angiogenesis and thrombosis. Proc Natl Acad Sci U S A **109**, 9342, 2012.